AIAA-90-0464

Continuous-Phase Properties of the Near-Injector Region of Non-Evaporating Pressure-Atomized Sprays

G. A. Ruff and G. M. Faeth
University of Michigan
Ann Arbor, MI

28th Aerospace Sciences Meeting
January 8-11, 1990/Reno, Nevada

For permission to copy or republish, contact the American Institute of Aeronautics and Astronautics
370 L'Enfant Promenade, S.W., Washington, D.C. 20024

CONTINUOUS-PHASE PROPERTIES OF THE NEAR-INJECTOR REGION OF NON-EVAPORATING PRESSURE-ATOMIZED SPRAYS

G. A. Ruff* and G. M. Faeth+
Department of Aerospace Engineering
The University of Michigan, Ann Arbor, Michigan

Abstract

Gas-phase properties in the dense-spray region of non-evaporating pressure-atomized sprays were studied—supplementing earlier work concerning the liquid-phase properties of this flow. The multiphase mixing layer that forms near the injector exit during atomization breakup was emphasized, considering large-scale (9.5 mm injector diameter) water jets injected vertically downward in still air at normal temperature and pressure. Mean and fluctuating gas velocities were measured using phase-discriminating laser velocimetry for dilute-spray conditions near the edge of the flow, and double-pulse holography for the dense-spray conditions near the liquid surface. The following general properties were observed for present test conditions: gas velocities are low in comparison to liquid velocities near the liquid surface; Weber numbers exceed drop breakup limits near the liquid surface, with this unstable region extending farther into the mixing layer when the liquid is initially turbulent since this promotes ejection of large liquid elements from the surface; and velocity differences between the phases are comparable to liquid velocities for much of the mixing layer, implying significant effects of separated flow. Scaling analysis, however, suggests reduced effects of separated flow when injector velocities and ambient pressures are increased from present test conditions—largely due to finer atomization.

Nomenclature

C_b	= drop breakup time coefficient
C_B	= aerodynamic breakup coefficient
C_c	= liquid core length coefficient
C_D	= drop drag coefficient
d	= injector exit diameter
d_p	= drop diameter
$d_{p_{av}}$	= average drop diameter for aerodynamic breakup
$d_{p_{cr}}$	= critical drop diameter for secondary breakup
k	= Favre-averaged turbulence kinetic energy
L	= injector passage length
L_c	= liquid core length
N	= number of measurements
Oh	= jet Ohnesorge number, $\mu_f/(\rho_f d\sigma)^{1/2}$
r	= radial distance
Re	= jet Reynolds number, $\rho_f u_0 d/\mu_f$
S	= separated flow factor, $(\tilde{u}_f - \tilde{u}_g)/\tilde{u}_f$
S_{bc}	= drop-breakup/liquid-core-residence time ratio, $\tau_{b_{cr}}/\tau_c$
S_{bp}	= drop breakup/response time ratio, $\tau_{b_{cr}}/\tau_{p_{cr}}$
S_c	= liquid-core-residence/drop-response time ratio, $\tau_c/\tau_{p_{cr}}$
S_f	= flow-residence/drop-response time ratio, $\tau_f/\tau_{p_{cr}}$
SMD	= Sauter mean diameter
t	= time
u	= streamwise velocity
v	= radial velocity
V	= volume of sample
We_{cr}	= critical Weber number for drop breakup, Eq. (3)
$\tilde{We}_g$	= Favre-averaged spray Weber number, Eq. (6)
We_{df}	= jet exit Weber number, $d\rho_f u_0^2/\sigma$
We_{xf}	= mixing layer Weber number, $x\rho_f u_0^2/\sigma$
x	= streamwise distance
μ	= molecular viscosity
ρ	= density
σ	= surface tension
τ_b	= drop breakup time, Eq. (18)
$\tau_{b_{cr}}$	= critical drop breakup time, Eq. (19)
τ_c	= liquid core residence time, Eq. (16)
τ_f	= flow residence time, Eq. (8)
τ_p	= drop response residence time, Eq. (10)
$\tau_{p_{cr}}$	= critical drop response residence time, Eq. (13)

Subscripts

cr	= properties at critical breakup condition
f	= liquid-phase property
g	= gas-phase property
p	= drop property
s	= liquid surface property
0	= injector exit condition

Superscripts

$\bar{(\ )}, (\ )'$	= time-averaged mean and root-mean-squared fluctuating quantities
$\tilde{(\ )}, (\ )''$	= Favre-averaged mean and root-mean-squared fluctuating quantities

Introduction

In order to reduce the time and cost of cut-and-try development of liquid-fueled combustors, there have been numerous efforts to develop methods to analyze spray processes. The present investigation seeks to contribute to the development of this methodology by studying the dense-spray region near the exit of the injector passage for pressure atomization processes. Experiments were limited to relatively large scale (9.5 mm injector diameter) nonevaporating round water jets injected into still air at normal temperatures and pressures. Earlier measurements of liquid volume fractions, entrainment rates, and dispersed-phase properties in the dense-spray region of these flows, reported by Ruff et al.,[1,2] were extended to provide gas-phase properties. The new measurements, along with additional information obtained from the data of Ruff et al.,[1] were used to continue study of locally-homogeneous-flow (LHF) analysis of the process, e.g., analysis based on the assumption of infinitely-fast interphase transport rates so that both phases have the same velocity and

---

* Graduate Assistant, currently Assistant Professor, Department of Mechanical Engineering, Drexel University, Philadelphia, Pennsylvania.

+ Professor, Fellow AIAA.

Copyright © 1990 American Institute of Aeronautics and Astronautics, Inc. All rights reserved.

are in thermodynamic equilibrium at each instant and point within the flow. Present measurements were limited to the atomization breakup regime where a multiphase mixing layer along the edge of the flow begins to develop right at the injector exit.[3,4] Jet exit conditions involved both slug flow and fully-developed turbulent pipe flow, since past work had shown sensitivity of dense spray properties to liquid-phase turbulence levels.[1,2]

Figure 1 is a sketch of the near-injector region for pressure-atomized injection in the atomization breakup regime.[5] The flow near the injector exit involves a liquid core surrounded by a multiphase mixing layer that begins to develop right at the injector exit for atomization breakup.[3,4] The dense-spray region is normally considered to include both the liquid core and the multiphase mixing layer up to the point where the liquid core disappears. There have been several studies of the length of the liquid core, taken as the length of unbroken liquid extending from the passage exit.[6-8] Findings indicate that this length is influenced by the breakup regime, turbulence properties at the injector exit and the gas/liquid density ratio. For atomization breakup of typical liquids in gases at atmospheric pressure, however, the dense-spray region extends quite far from the injector, ca. 200-400 injector diameters. Thus, dense sprays are an important feature of spray injection processes due both to their extent and their influence on drop properties at the start of the dilute-spray region.

The multiphase mixing layer is also affected by the breakup regime, jet exit turbulence properties and the density ratio of the flow.[1,2,9-11] Ruff et al.[1] provide information on liquid-phase properties in the multiphase mixing layer for water jets in still air at atmospheric pressure, using double-pulse holography to find liquid element (drop) sizes and velocities. It was found that the multiphase mixing layer was relatively dilute above the liquid surface, for their test conditions, with liquid volume fractions generally less than 1 percent. The inner portion of the mixing layer contained large irregularly-shaped liquid elements and drops while the proportion of spherical drops increased and drop sizes decreased with increasing radial distance, suggesting significant effects of secondary breakup in the flow. The velocities of large drops were generally much larger than small drops, implying separated flow effects were important as well. Increased turbulence levels at the jet exit had a substantial effect on the structure of the flow, increasing the number and size of irregular liquid elements by promoting ejection of liquid from the liquid surface, and increasing the width of the liquid-containing region of the multiphase mixing layer. Wu et al.,[9] also observed significant effects of jet exit conditions on the rate of spread of the outer edge of the multiphase mixing layer.

The complexities of dense sprays—involving stripping of liquid from the all-liquid core, the presence of irregular liquid elements, secondary breakup, and turbulent dispersion of drops toward the edge of the flow—makes the LHF approximation attractive as a means of circumventing detailed descriptions of these phenomena. Ruff et al.[2] found that LHF predictions were reasonably effective for estimating distributions of liquid volume fractions for atomization breakup in the region where mean liquid volume fractions were greater than 0.2. As noted earlier, however, the multiphase mixing layer which dominates flow properties at lower liquid volume fractions, exhibits significant effects of separated flow and limits the effectiveness of the LHF approximation for these test conditions.[1] Other evaluations of the LHF approximation find varying degrees of success—at times yielding encouraging results and at other times overestimating the rate of development of the flow as the spray becomes dilute.[5,9-12] Unfortunately, methods for determining conditions when use of the LHF approximation is appropriate for dense sprays have not been developed. The main difficulty is that success of the LHF approximation depends on drops being small enough to respond quickly to changes in gas properties, while information on both drop sizes and gas properties in dense sprays is very limited.

The objective of the present investigation was to seek a better understanding of the properties of dense sprays by studying gas-phase velocities in the multiphase mixing layer for the same test conditions as Ruff et al.[1,2] Coupled with the existing measurements of liquid-phase properties (drop sizes and velocities), this provides a relatively complete picture of the structure of these flows. Furthermore, knowledge of both liquid- and gas-phase velocities allows direct evaluation of the propensity for secondary drop breakup as well as quantitative estimates of effects of separated flow. Mean and fluctuating gas velocities near the edge of the multiphase mixing layer were measured using phase-discriminating laser velocimetry (LV); while double-pulse holography was used near the liquid surface where LV was no longer feasible. Similar to earlier work,[1,2] the measurements were compared with predictions based on the LHF approximation to help provide a measure of separated-flow effects. Characteristic time considerations of drop breakup and response were also used to interpret dense-spray properties and gain a better understanding of conditions where use of the LHF approximation is appropriate.

The paper begins with descriptions of experimental methods and the approach used for the LHF computations. Experimental results are then described, considering mean and fluctuating phase velocities, drop breakup parameters, and separated-flow parameters. The paper concludes with consideration of characteristic times of various processes in the flow in order to find conditions where use of the LHF approximation is appropriate. The present discussion is brief, additional details and a complete tabulation of data can be found in Ruff.[13]

Experimental Methods

Apparatus

The experimental apparatus was identical to past work,[1,2] and will only be described briefly. The arrangement involved large-scale (9.5 mm injector diameter) water jets injected vertically downward in still air at normal temperature and pressure. City water was supplied to the injector by a centrifugal pump, collected in a baffled tub and discharged to a drain. The water flow rate was measured with a paddle-wheel flow meter that was calibrated by collecting water for timed intervals.

The slug and fully-developed flow injectors were also identical to Ruff et al.[1,2] Measurements of mean and fluctuating velocities across the exit of the injectors,[13] showed that the slug flow injector provided relatively uniform velocities, with a streamwise turbulence intensity of roughly 1 percent, at the jet exit; while the fully-developed flow injector yielded jet exit properties that approximated existing measurements for fully-measured by traversing the injector, since instrumentation was mounted rigidly. Positioning accuracies were 5 μm in the horizontal direction and 0.5 mm in the vertical direction.

Instrumentation

Laser Velocimetry. Present measurements were limited to mean and fluctuating gas velocities using phase-discriminating laser velocimetry (LV) and mean gas velocities using double-pulse holography. The ambient air was seeded with condensed oil particles having diameters less than 1 μm for LV measurements. The seeding particles have a flat frequency response to the gas motion up to about 30 kHz for present conditions, which was adequate for the region where LV measurements were made. A large enclosure (3 × 3 × 4 m high) was constructed around the spray facility to avoid contaminating laboratory equipment with seeding particles. For an enclosure of this size, the induced counterflow velocity is

less than 2 percent of the axial velocities in the region measured near the edge of the jets.

A phase-discriminating LV system, along the lines of Modarress et al.,[16] was used to avoid biasing gas phase velocity signals with liquid velocity signals. A sketchy of the arrangement appears in Fig. 2. The LV signal was obtained using the green line (514.5 nm) of an argon-ion laser (4W, Coherent, INNOVA 90-4) in the dual-beam forward-scatter mode. A 3.75:1 beam expander was used to minimize the dimensions of the measuring volume and to improve signal-to-noise ratios in the adverse environment of the multiphase mixing layer. The plane of the LV beams was rotated to measure both streamwise and crosstream velocities. The LV was frequency shifted (40 MHz Bragg cell, TSI model 9180-12) to eliminate effects of directional bias and ambiguity. The receiving optics observed the probe volume of the LV at an angle of 30° from the forward-scattering direction. This arrangement yielded a measuring volume having a diameter of 60 μm and a length of 110 μm.

The phase-discrimination system involved surrounding the LV measuring volume with the beam from a 5 mW HeNe laser directed at an angle of 15° from the LV axis, with collection optics in the forward-scattering direction also at an angle of 15° from the LV axis. This yielded a region viewed by the discriminator system that had a diameter of 0.6 mm and a length of 1.3 mm, surrounding the LV measuring volume as shown in the inset of Fig. 2. Thus, droplets that could graze or cross the LV measuring volume yielded a scattering signal on the discriminator output so that velocities recorded when drops were present could be eliminated from the velocity record.

The LV scattering signal was recorded using a photomultiplier (TSI model 9160) and processed using a burst counter (TSI model 1990 C). The measurements involved low burst densities (one seeding particle in the measuring volume) and high data densities (time between validated velocity signals small in comparison to integral time scales); therefore, the analog output of the processor was time averaged to yield unbiased time averages. This involved low-pass filtering (Ithaco model 4213) the output signal before it was digitized (LeCroy models 8212A/8 and 8800A) and transferred to a microcomputer (IBM AT) for processing and storage.

The performance of the phase-discriminator system was checked by measuring LV data rates with and without seeding particles present. It was required that the LV data rate at least double for the measurements to be considered valid. Additionally, no measurement was accepted if more than 40 percent of the LV signal was rejected due to signals from the phase discriminator system. Calibration of this approach, using velocities of small particles measured by double-pulse holography, indicated significant bias of LV gas velocity measurements if these limits were exceeded.

LV signals were averaged for two minutes to provide repeatable values of mean and fluctuating gas velocities. Experimental uncertainties (95 percent confidence) are estimated to be less than 8 percent for mean streamwise velocities,and less than 15 percent for streamwise and crosstream velocity fluctuations, largely dominated by finite sampling times. Measurements were repeatable well within these limits.

Double-Pulse Holography. LV data rates from drops alone became unacceptably high near the liquid surface. Therefore, measurements were made in this region using double-pulse holography. This approach is tedious and somewhat less accurate, due to difficulties in accumulating sufficient velocity samples and reduced particle response since only particles having diameters of roughly 5 μm and greater could be measured. Nevertheless, holography provided access to portions of the multiphase mixing layer that were no longer feasible using LV.

Holography methods were the same as Ruff et al.[1] An off-axis holographic arrangement was used, based on the Spectron Development Laboratories model HTRC-5000 system. This involved passing a 10 mm diameter object beam through the spray, and then expanding it back to the 85 mm diameter of the reference beam to form the hologram. The holograms were created using a ruby laser that deposited 50 mJ in 20 ns which effectively stopped the flow so that drops as small as 5 μm could be sized. The laser could be double pulsed with separation times as small as 2 μs, to yield two images of the flow upon reconstruction so that velocities could be measured. The separation time between the two pulses of the laser was measured with a LeCroy model 9400 digital oscilloscope. Directional ambiguity was eliminated by using pulses of unequal intensity, since the pulse with the greater intensity yields a higher contrast reconstructed image.[17] The holograms were obtained in a darkened room using AGFA 8E75HD-NAH unbacked holographic plates with a 100 × 125 mm film format.

The holograms were reconstructed using a 15 mW HeNe laser with the beam expanded to a diameter of 60 mm and passed through the hologram. This yielded a real image of the spray in front of the hologram. The properties of small particles in the spray were observed with an MTI model 65 video camera with optics to provide a field of view of 1 × 1.2 mm within the spray. Computer controlled x-y traversing of the hologram (1 μm resolution) and z traversing of the camera (5 μm resolution) allowed the region crossed by the object beam to be studied. The video image was analyzed using a Gould FD5000 Image Processing System. Reference pins in the object field provided both size and position calibrations.

Velocity data was obtained over 6 × 6 × 4 mm volumes, using at least three holograms per position. The data was spatially averaged over the width of the measuring volumes, or ± 1/2 the distance between adjacent radial positions, whichever was smaller. Velocity measurements were based on the motion of the centroid of the image and were correlated as a function of diameter using a least squares fit, considering drops having diameters less than 30 μm for present estimates of gas velocities. This typically involved correlation of 50-150 individual velocity determinations. The value given by the fit at a diameter of 5 μm, which is the lower end of the range that could be resolved, was used as the estimate of mean gas velocities. Unfortunately, sample sizes were too small to obtain reliable estimates of velocity fluctuations.

Gradient broadening errors of mean gas velocities were not very significant for present conditions. Similarly, bias errors for slug flow conditions are also felt to be small, since the small particles were generally formed at the liquid surface and had time to equilibriate to gas velocities in the region where measurements were made. However, bias errors are more significant for fully-developed injector exit conditions where secondary breakup is more important and small drops were probably observed in a relatively short time after breakup before they could relax to gas velocities in some instances—this will be discussed later. Excluding potential effects of bias for fully-developed injector exit conditions, experimental uncertainties (95 percent confidence) are estimated to be less than 30 percent, largely governed by sampling limitations.

Test Conditions. The experiments involved both fully-developed turbulent pipe flow and slug flow jet exit conditions in the atomization breakup regime, the same as the conditions considered by Ruff et al.[1] This involved a mean jet exit velocity of 56.3 m/s, yielding other jet exit parameters as follows: Reynolds number, 534000; Weber numbers based on gas and liquid densities, 500 and 412000, respectively; and Ohnesorge number, 0.00121. Under existing criteria from Ranz[3] and Miesse,[4] these conditions are well within the

atomization breakup regime and properly yielded a multiphase mixing layer that began at the exit of the injector.

Theoretical Methods

Predictions of flow properties were drawn from Ruff et al.[1] These results are based on the use of the LHF approximation while neglecting evaporation of the liquid. This implies that the ambient air is saturated with water vapor, which was formally not the case, however, effects of evaporation are negligible for present test conditions.[1] Other major assumptions of the analysis are as follows: steady (in the mean) axisymmetric flow with no swirl; negligible kinetic energy and viscous dissipation of the mean flow; buoyancy only affects the mean flow; equal exchange coefficients of all species and phases; and negligible mass transport between the phases. Under these assumptions, the flow field can be found using a simplified version of the conserved-scalar formalism of Lockwood and Naguib[18] but based on mass-weighted (Favre) averages, following Bilger.[19] Governing equations are solved for conservation of mass, streamwise mean momentum, mean mixture fraction, turbulence kinetic energy and the rate of dissipation of turbulence kinetic energy. Since the two phases do not exchange mass, all scalar properties can be found from the Favre-averaged mixture fraction and it is not necessary to solve a governing equation for mean-squared mixture fraction fluctuations.[1] Initial conditions were based on the LV velocity measurements of jet properties at the injector exit,[13] supplemented by available information on the properties of fully-developed turbulent pipe flows when appropriate,[14,15] as described by Ruff et al.[1]

The governing equations and all empirical constants are summarized elsewhere.[1,5] Justification of the assumptions of the analysis (except for the LHF approximation which is to be studied), details of the numerical computations, and estimates of numerical accuracy, are discussed by Ruff et al.[1] The use of turbulence models to predict the mixing properties of turbulent flows is naturally open to question, however, the present jet-like boundary layer configuration provides conditions where turbulence models perform reasonably well. In particular, the formulation has been successfully calibrated for a variety of constant- and variable-density single-phase round jets.[20] Additionally, the same formulation has been used successfully to estimate the structure of turbulent round air jets injected into water, which involves the same density ratio as the present flow.[21] Thus, the main issue of the present evaluation is the adequacy of the LHF approximation for estimating the properties of the near-injector region for liquid injection into gases.

Results and Discussion

Phase Velocities. Measured mean velocities in the multiphase mixing layer for slug and fully-developed flow jet exit conditions are illustrated in Figs. 3 and 4. Velocities, normalized by the mean jet exit velocity, are plotted as a function of r/x, the radial similarity variable for turbulent jets, at x/d = 12.5, 25, 50 and 100. The radial similarity variable is only chosen for convenience to indicate the width of the flow, flow properties do not exhibit similarity in the r/x coordinate system. Three sets of velocity measurements are shown: continuous (gas)-phase mean velocities found using the phase-discriminating LV; dispersed (drop)-phase mean velocities for 5 μm diameter particles, measured using double-flash holography (which are taken to be representative of mean gas-phase velocities in the region where LV was no longer feasible); and Favre-averaged velocities of the mixture as a whole for comparison with predictions. The Favre-averaged velocities were found by summing over a sample volume V, containing N drops, as follows:

$$\tilde{u} = \frac{\sum_{i=1}^{N}(\pi/6)\rho_f d_{pi}^3 u_{pi} + (V - \sum_{i=1}^{N}(\pi/6)d_{pi}^3)\rho_g \bar{u}_g}{\sum_{i=1}^{N}(\pi/6)\rho_f d_{pi}^3 + (V - \sum_{i=1}^{N}(\pi/6)d_{pi}^3)\rho_g} \quad (1)$$

where drop size and velocity determinations included the full range of the data reported by Ruff et al.[1] Mean gas velocities in Eq. (1) were obtained from either the LV or the holography measurements (based on 5 μm diameter drops). The range of positions of the liquid surface, observed using holography, is indicated by the cross-hatched regions in the figures. Finally, LHF predictions of Favre-averaged velocities are also illustrated on the plots. Two predictions are shown for slug flow, ignoring and allowing for boundary layer development along the walls of the injector passage, the latter using a flow development length of L/d = 5. These limits should bound the properties of the slug flow injector; however, differences between the two predictions are not very significant.

The results for slug flow jet exit conditions, Fig. 3, exhibit reasonably good agreement between mean velocity measurements found by LV and particle tracking in the region where they overlap. Gas velocities remain quite low in the mixing layer, and only increase slightly near the liquid surface as distance from the injector exit increases. Near the injector exit, Favre-averaged velocities are significantly greater than gas velocities except near the outer edge of the mixing layer. Farther from the injector, however, differences between phase velocities are only significant near the liquid surface. Nevertheless, separated-flow effects are important throughout the mixing layer and LHF predictions of mean velocities are not satisfactory.

The results for the fully-developed jet exit conditions, Fig. 4, exhibit greater differences between mean velocities found by LV and particle tracking than for slug flow jet exit conditions. In general, velocities measured by particle tracking are biased upward from the LV results. This is felt to be the result of the breakup of larger liquid elements that are more common for fully-developed flow than for slug flow, generating small drops with relatively high initial velocities. Measurement of the velocity of these drops before they relax to the gas velocity would tend to bias present velocity measurements toward higher velocities. The extent of this effect is difficult to quantify; therefore, the particle velocities of Fig. 4 are at best representative of an upper bound on gas velocities. Similar to slug flow, gas velocities remain relatively low throughout the mixing layer, Favre-averaged velocities are generally significantly greater than gas velocities indicating significant effects of separated flow, and LHF predictions are not very satisfactory as a result.

Measured and predicted gas phase velocity fluctuations are illustrated in Figs. 5 and 6 for slug and fully-developed flow jet exit conditions. The measurements are limited to streamwise and radial velocity fluctuations found by LV, which generally only covers the outer half of the mixing layer. Predictions are based on the isotropic approximation, $\tilde{u}''^2 = \tilde{v}''^2 = 2k/3$, and are Favre averages under the LHF assumption. Measured velocity fluctuations are nearly isotropic near the outer edge of the mixing layer, which is similar to the behavior of single-phase jets. Streamwise velocity fluctuations are substantially greater than radial velocity fluctuations, however, as the spray becomes dense (this is particularly evident for x/d = 12.5). Such behavior is typical of dense sprays in regions where relative velocities are significant.[5,22,23] Other than indicating that velocity fluctuations should increase in the dense portions of the mixing layer, in a qualitative way, the LHF predictions of velocity fluctuations are not very useful.

Liquid Breakup. The availability of liquid-phase properties from Ruff et al.,[1] and gas-phase velocities from the present study, allows consideration of liquid breakup phenomena in the dense-spray region. Two phenomena are of interest: primary drop formation at the liquid surface and secondary drop breakup within the mixing layer.

Reitz[24] and Reitz and Bracco[25] have proposed a formula to estimate drop sizes due to primary drop formation at the liquid surface. The approach is based on Taylor's[26] theory of aerodynamically induced growth of surface waves for a nonturbulent liquid, taking the average diameter of drops formed at the surface to be proportional to the wavelength of unstable surface waves. Present test conditions involve $(\rho_f/\rho_g)(Re/We_f)^2 > 1$; at this condition the expression for the average drop diameter due to primary drop breakup becomes:[24,25]

$$d_{p_{av}} = 6\pi C_B\sigma/(\rho_g(u_o - \bar{u}_{gs})^2) \qquad (2)$$

where C_B is the constant of proportionality which is thought to have a magnitude near unity. In Eq. (2), liquid surface velocities have been taken equal to the mean velocity at the jet exit; this is reasonable for present test conditions, based on measurements of the velocity of protuberances from the liquid surface as well as estimates from the LHF predictions.

The estimates of $d_{p_{av}}$ from Eq. (2) are summarized along with measured SMD near the liquid surface in Table 1 for both slug and fully-developed flow jet exit conditions. Gas velocities near the liquid surface are listed in the table, based on measured velocities of 5 μm diameter drops. Average drop diameters from Eq. (2) were computed using $C_B = 0.5$, which provides a rough match of measured SMD for slug flow jet exit conditions, where the liquid is nonturbulent and corresponds to the conditions of Taylor's[26] analysis. Except for x/d = 50, where sampling limitations may be a factor, Eq. (2) provides an estimate of SMD near the surface that is within experimental uncertainties for slug flow conditions. However, measured drop sizes near the surface are 4-6 times larger than the estimates of Eq. (2) for fully-developed flow jet exit conditions. This is caused by enhanced liquid ejection due to distortion of the liquid surface by liquid-phase turbulence—a mechanism that is not considered by the aerodynamic breakup theory.

There are numerous criteria in the literature for estimating secondary breakup conditions of drops. These are frequently stated in terms of a critical Weber number based on gas density, defined as follows:

$$We_{cr} = (\rho_g d_p(u_p-u_g)^2/\sigma)_{cr} \qquad (3)$$

One criterion, discussed by Clift et al.,[27] is based on measurements of water drops accelerated by shock waves, yielding:

$$We_{cr} = 6.5 \qquad (4)$$

Another criterion, discussed by Pruppacker and Klett,[28] was obtained for liquid drops falling in still air and has the following form:

$$We_{cr} = 8 / C_D \qquad (5)$$

For present test conditions, droplet drag coefficients are in the range 0.8-1.2, based on the standard drag curve for spheres;[5] therefore, Eqs. (4) and (5) yield similar values of We_{cr}.

In order to quantify the potential for secondary drop breakup in the mixing layer, a mass-weighted Weber number was computed at each point in the sprays where drop size and velocity measurements were available from Ruff et al.[1] Given N drop measurements at a particular location, the mass-weighted Weber number was computed as follows:

$$We_f = \sum_{i=1}^{N} (\rho_g d_p(u_p-\bar{u}_g)^2/\sigma)_i d_{pi}^3 \Big/ \sum_{i=1}^{N} d_{pi}^3 \qquad (6)$$

The resulting distributions of $\tilde{We}_g$ for the sprays having slug and fully-developed jet exit conditions are plotted in Fig. 7. For reference purposes, the range of positions of the liquid surface are also shown on the plots. The values of $\tilde{We}_g$ are greatest near the liquid surface and decrease monotonically with increasing distance from the surface. In general, values of $\tilde{We}_g$ near the liquid surface exceed the values of We_{cr} for breakup from Eqs. (4) and (5), supporting the probability of significant effects of secondary breakup in the mixing layer. The larger liquid elements ejected from the surface when the liquid is turbulent cause $\tilde{We}_g$ to remain above critical values farther across the mixing layer than for a nonturbulent liquid core, implying greater effects of secondary breakup for these conditions. In view of these findings, and the small liquid volume fractions, it appears that secondary breakup rather than drop collisions is a dominant feature of the dense spray portion of the mixing layer for present test conditions.

Direct indications of secondary drop breakup were occasionally observed on the hologram reconstructions. No instance of bag-type breakup was observed, perhaps because this mode of breakup only occurs for a relatively narrow range of Weber numbers,[5] so that the probability of observing it from single-pulse holograms is relatively small. However, indications of stripping-type breakup, discussed by Ranger and Nicholls,[29] were observed. A typical sketch of stripping drop breakup, prepared from a single-pulse hologram of the event, appears in Fig. 8. This involves a large drop with wave-like disturbances along the surface, followed by a trail of smaller drops. Distortion near the downstream end of the parent drop suggests that the next drop in the stream is about to be formed. This type of breakup appears to be caused by Kelvin-Helmholtz instabilities, originating near the forward stagnation point of the parent drop and propagating around its surface to the near stagnation point, where the instability causes a smaller drop to separated from the parent drop.

A second type of secondary breakup that was observed is also sketched in Fig. 8. This involves ligament-type breakup due to the elongation of high aspect ratio ellipsoidal elements or ligaments, causing them to separate into two or more smaller drops. Since present mean gas velocities are small and relatively uniform (see Figs. 3 and 4), this type of breakup doesn't appear to be due to differential distortion by varying shear forces from the gas phase. More likely explanations involve either differential velocities present within the elongated liquid element when it was ejected from the surface that cannot be stabilized by surface tension forces, or Rayleigh instability of ligaments.

Separated-Flow Effects. Although the results illustrated in Figs. 3 and 4 provide an indication of relative velocities between the phases, these figures are somewhat misleading since small velocities near the edge of the flow give the impression that separated flow effects are small in this region as well. This is not the case, which can be seen by plotting a Favre-averaged separated-flow factor, defined as follows:

$$S = (\tilde{u}_f - \tilde{u}_g) / \tilde{u}_f \qquad (7)$$

Distributions of S are illustrated in Fig. 9 for both slug and fully-developed jet exit conditions. High values of S, approaching unity, are observed throughout the mixing layer near the jet exit, and near the liquid surface for all streamwise

positions. However, values of S near the outer edge of the flow tend to decrease with increasing distance from the injector, approaching values in the range 0.1-0.2 for fully-developed jet exit conditions at x/d = 100. In spite of the presence of larger drops near the liquid surface, values of S are generally lower for fully-developed than slug flow jet exit conditions.

The trends seen in Fig. 9 result from both the generation of drops at the liquid surface and momentum exchange between the phases in the mixing layer. Velocities within the liquid core remain near liquid injection velocities so that newly-formed drops near the injector exit and along the liquid surface generally have velocities that are significantly greater than gas velocities, yielding relatively large values of S. Drops near the outer edge of the flow, however, must have had significant residence times in the gas so that turbulent dispersion can transport them to this region. Therefore, drops near the edge of the flow tend to relax toward gas velocities particularly when residence times are long, e.g., at large x/d. Additionally, fully-developed jet exit conditions increase drop concentrations in the mixing layer in comparison to slug flow exit conditions, causing greater acceleration of the gas within the mixing layer. This compensates for the higher velocities associated with larger drops produced by fully-developed exit conditions and tends to reduce S. Nevertheless, with values of S on the order of unity throughout most of the mixing layer, separated-flow effects are clearly important which explains why predictions based on the LHF approximation are poor for present test conditions.

Characteristic Times. Present results suggest that effects of separated flow and secondary breakup are important in the dense-spray region. However, these results have only been established for a single mean jet velocity and ambient environment. Thus, some characteristic time considerations are undertaken in the following in order to provide more insight concerning effects of separated flow and secondary breakup and to help relate present results to practical pressure-atomized sprays.

The potential importance of separated flow in the mixing layer can be evaluated by comparing characteristic response times of the flow and the drops. An appropriate characteristic response time for the mixing layer is the residence time required to reach any streamwise position. The momentum of the liquid dominates the present flow while velocities in the all-liquid core do not change very much with streamwise distance. Furthermore, the velocities of the largest drops, which are most prone to separated-flow effects, are approximately the same as the injector velocity based on the measurements of Ruff et al.[1] Therefore, an appropriate characteristic flow residence time for the mixing layer can be based on the mean streamwise velocity at the jet exit, as follows:

$$\tau_f = x / u_o \tag{8}$$

The characteristic response time of drops varies, with the largest drops having the longest response times. Use of the aerodynamic breakup expression for the average drop size formed at the liquid surface, Eq. (2), offers one possibility for estimating maximum drop sizes. However, the results of Table 1 show that this would underestimate drop sizes when the liquid core was turbulent. A more general approach is suggested by the results of Fig. 7, where it is seen that the largest drops are comparable to the maximum drop size at We_{cr} for both slug and fully-developed jet exit conditions. Assuming that gas velocities are small and taking the jet exit velocity to be representative of the velocities of the largest drops, which is reasonable from the results illustrated in Figs. 3 and 4, the following estimate of maximum drop sizes in the mixing layer is obtained:

$$d_{p_{cr}} = \sigma We_{cr} / (\rho_g u_o^2) \tag{9}$$

Notably, except for a different constant of proportionality, the secondary breakup criterion of Eq. (9) is identical to the primary aerodynamic breakup criterion for the liquid surface given by Eq. (2).

A characteristic response time for drops can be defined in terms of their rate of deceleration, as follows:

$$\tau_p = -1 / (du_p/dx) = -u_p / (du_p/dt) \tag{10}$$

Virtual mass and Basset history forces can generally be ignored when computing drop motion in sprays since liquid densities are usually significantly greater than gas densities.[5] Furthermore, pressures within the mixing layer are constant. Thus, conservation of momentum for a drop yields:[5]

$$du_p/dt = -3 \rho_g C_D (u_p - u_g)^2 / (4 \rho_f d_p) \tag{11}$$

Streamwise velocities have been assumed to be large in comparison to crosstream velocities in arriving at Eq. (11); this is justified due to the boundary-layer character of the mixing layer. Substituting Eq. (11) into Eq. (10) then yields an expression for the response time of a drop having a diameter d_p, as follows:

$$\tau_p = 4 \rho_f d_p u_p / (3 \rho_g C_D (u_p - u_g)^2) \tag{12}$$

Finally, assuming $u_g << u_p$ and taking $u_p \approx u_o$, as before, and using Eq. (9) to identify the characteristic drop diameter, the characteristic drop response time becomes:

$$\tau_{p_{cr}} = 4 We_{cr} \rho_f \sigma / (3 C_D \rho_g^2 u_o^3) \tag{13}$$

Since We_{cr} is roughly a constant while C_D does not vary appreciably for drops in sprays,[5] Eq. (13) shows that increased gas densities and injector exit velocities cause substantial reductions of drop response times, both through the effects of breakup which reduces drop sizes and relative increases of drag in comparison to inertia of the drops for a particular drop size (see Eq. (12)).

The effects of separated flow can be indicated by forming the ratio of the characteristic response times of the drops and the flow, yielding a separated-flow factor, S_x, defined as follows:

$$S_x = \tau_f / \tau_{p_{cr}} = \left(\frac{3 C_D}{4 We_{cr}} \right) \left(\frac{\rho_g}{\rho_f} \right)^2 \left(\frac{x \rho_f u_o^2}{\sigma} \right) \tag{14}$$

where the last factor on the RHS of Eq. (14) can be recognized to be the Weber number based on the dimension x and the liquid density, $We_{xf} = x \rho_f u_o^2 / \sigma$. Large values of S_x correspond to regions of the mixing layer where separated flow effects become small. The distance, x, in Eq. (14) should be interpreted as the relaxation distance required from the point when a particular critical-sized drop appears in the flow.

For present flows, drops continue to be formed at the liquid surface throughout the region where measurements were made. Therefore, relaxation distances remain small near the liquid surface yielding small values of S_x from Eq. (14) in this region. This is consistent with the large relative velocity parameters in Fig. 10 near the liquid surface. Drops near the edge of the flow originate near the injector exit. In this case, taking $C_D = 1$ and $We_{cr} = 10$, Eq. (14) yields values of S_x increasing with distance and roughly in the range 1-4 for x/d in

the range 25-100. This implies significant effects of separated flow near the jet exit, with separated-flow effects decreasing near the edge of the flow at larger streamwise distances, generally as observed in Fig. 9.

Based on these results, S_x defined in Eq. (14) appears to be a reasonable measure of separated flow effects in the mixing layer. This implies that the dense-spray region tends toward LHF flow at the limit of large We_{xf}, with approach to this limit being more rapid when the density ratio, ρ_g/ρ_f, is increased. For a given fluid and ambient gas, this implies approach to LHF flow at high liquid injection velocities and ambient densities, at least for regions of these flows not too near the jet exit and the liquid surface. Recall, however, that Eq. (14) was based on the assumption that gas velocities are low in comparison to the liquid surface velocity and the velocity of large liquid elements that tend to break up. This limits application of Eq., (14) to the region where the gas-phase velocity profile is developing. The extent of this region is expected to decrease as separated-flow effects become smaller and the velocity field behaves more like the LHF velocity distributions illustrated in Figs. 3 and 4.

It is also of interest to assess effects of separated flow over the length of the liquid core, which serves as a measure of the length of the dense-spray region. Taylor's[26] aerodynamic breakup analysis yields the following expression for the length of the liquid core:

$$L_c/d = C_c\,(\rho_f/\rho_g)^{1/2} \tag{15}$$

Chehroudi et al.[8] find C_c in the range 7-16 for pressure-atomized round jets in still gases for the atomization breakup regime, the high value being based on their measurements and the low value on the measurements of Hiroyasu et al.[7] Taking the characteristic velocity of large drops to be u_o, as before, a characteristic residence time for the liquid core becomes:

$$\tau_c = L_c/u_o = C_c(d/u_o)(\rho_f/\rho_g)^{1/2} \tag{16}$$

Forming a liquid-core-residence/drop-response time ratio, and obtaining the characteristic drop response time from Eq. (13), then yields:

$$S_c = \tau_c/\tau_{p_{cr}} = \left(\frac{3\,C_cC_D}{4\,We_{cr}}\right)\left(\frac{\rho_g}{\rho_f}\right)^{3/2}\left(\frac{d\rho_f u_o^2}{\sigma}\right) \tag{17}$$

where the last factor on the RHS of Eq. (17) is the Weber number based on the injector diameter and the liquid density, $We_{df} = d\rho_f u_o^2/\sigma$.

As before, a large value of S_c implies relatively small effects of separated flow in the dense spray region. Comparing S_c from Eq. (17) with S_x from Eq. (14) shows that the effect of the density ratio of the flow is somewhat reduced for S_c. This occurs since the length of the liquid core decreases as the gas density increases through Eq. (15) so that there is less residence time available in the mixing-layer when ambient densities are high. Equations (16) and (17) also indicate a strong effect of injector passage diameter since the length of the liquid core scales directly with the injector diameter. This implies that small diameter injectors may still be subject to significant separated flow effects near the downstream end of the dense-spray region, even at high ambient pressures. Similar to considerations for S_x, however, Eq. (17) suggests approach to LHF conditions at large We_{df}, with this approach being more rapid when ρ_g/ρ_f is large.

In addition to characteristic residence times associated with primary breakup and liquid removal from the all-liquid core, the time required for secondary breakup is an important feature of the mixing layer. The ligament-type breakup observed during present tests is associated with primary breakup at the liquid surface and is likely to be relatively fast. Therefore, only stripping-type breakup, involving a high-speed drop gradually decreasing in size by smaller drops being stripped from its surface, will be considered in the following. Ranger and Nicholls,[29] provide the following correlation for the breakup time by this mechanism:

$$\tau_b = C_b d_p(\rho_f/\rho_g)^{1/2}/(u_p-u_g) \tag{18}$$

where the empirical factor $C_b \approx 4$. Taking the maximum stable drop size from Eq. (9) to represent the characteristic drop breakup time, and adopting the approximations $u_g << u_p$ and $u_p \approx u_o$ as before, then yields:

$$\tau_{b_{cr}} = C_b We_{cr}\sigma(\rho_f/\rho_g)^{3/2}/(\rho_f u_o^3) \tag{19}$$

A variety of characteristic response time ratios can be formed using Eq. (19), but two are of particular interest: $\tau_{b_{cr}}/\tau_{p_{cr}}$ and $\tau_{b_{cr}}/\tau_c$. Forming the first ratio from Eqs. (13) and (19) yields:

$$S_{bp} = \tau_{b_{cr}}/\tau_{p_{cr}} = \left(\frac{3\,C_b\,C_D}{4}\right)\left(\frac{\rho_g}{\rho_f}\right)^{1/2} \tag{20}$$

Small values of S_{bp} imply that breakup times are small in comparison to the time required for drops having the critical diameter for breakup to relax toward the local gas velocity. Such conditions are actually necessary for Eq. (18) to be appropriate. Furthermore, values of S_{bp} provide a relative measure of the rate controlling capabilities of drop breakup and drop drag on the properties of the mixing layer. Taking $C_b = 4$ from Ranger and Nicholls,[29] and $C_D \approx 1$ as before, yields S_{bp} ca. 0.1 for present test conditions which indicates that breakup of large drops is relatively fast. At high pressures, however, larger values of S_{bp} would be reached so that breakup processes would extend over distances comparable to those required for drops to decelerate toward local gas velocities. This implies that drop breakup would have to be treated as a finite-rate process, analogous to the effect of drag on drop motion.

Another perspective on drop breakup phenomena can be found by forming the ratio $\tau_{b_{cr}}/\tau_c$ in order to obtain a measure of secondary breakup times to residence times in the mixing layer. This ratio can be obtained from Eqs. (16) and (19) as follows:

$$S_{bc} = \tau_{b_{cr}}/\tau_c = \left(\frac{C_b We_{cr}}{C_c}\right)\left(\frac{\sigma}{d\rho_g u_o^2}\right) \tag{21}$$

A more convenient form to evaluate S_{bc} for present test conditions can be found by introducing $d_{p_{av}}$ from Eq. (2) into Eq. (21), yielding:

$$S_{bc} = \left(\frac{C_b We_{cr}}{6\pi C_B C_c}\right)\left(\frac{d_{p_{av}}}{d}\right) \tag{22}$$

The first factor on the RHS of Eq. (22) is approximately one-half while $d_{p_{av}}$ is summarized in Table 1 for various points

along the mixing layer of the present flows. This yields S_{bc} ca. 0.01, implying that secondary breakup occurs over distances that are short in comparison to the length of the liquid core. This is consistent with the stripping-type drop breakup process illustrated in Fig. 8 and is mainly the result of the large injector diameters used during the present experiments. The flow for smaller injector diameters, typical of most practical applications, however, would involve values of S_{bc} nearer unity where secondary breakup would become a significant rate-controlling step within the dense spray region. Consideration of Eq. (21) shows that S_{bc} tends to decrease as pressure increases as well; therefore, the relative importance of secondary breakup, like most aspects of dense sprays, must be evaluated on a case-by-case basis.

Conclusions

The multiphase mixing layer in the near-injector region of pressure-atomized sprays was investigated, considering both slug and fully-developed flow at the jet exit. The major conclusions of the study are as follows:

1. For present test conditions, the dispersed-flow region of the multiphase mixing layers was surprisingly dilute (liquid volume fractions less than 1 percent); was dominated by breakup and separated-flow processes while effects of collisions appear to be small; and was strongly influenced by the presence of liquid turbulence.

2. Use of the locally-homogeneous-flow approximation was not very effective for estimating the properties of the multiphase mixing layers for present test conditions, since large drops are continuously ejected from the liquid surface and require significant residence times to relax to gas velocities in the flow. Residence-time considerations imply that locally-homogeneous flow corresponds to a large We_{fx} or We_{fd} limit, with this limit approached more rapidly as the density ratio of the flow, ρ_g/ρ_f, increases.

3. For slug flow jet exit conditions, SMD along the liquid surface are roughly equal to estimates of the average drop diameter for aerodynamic breakup proposed by Reitz[24] and Reitz and Bracco[25] (using $C_B \approx 0.5$). In contrast, the presence of liquid-phase turbulence due to fully-developed flow jet exit conditions yielded drop sizes several times larger than aerodynamic breakup estimates, since liquid turbulence promotes distortion of the liquid surface. Nevertheless, maximum stable drop sizes for secondary breakup are comparable to drop sizes for aerodynamic breakup, so that drop sizes are not very different for slug and fully-developed jet exit conditions in the region away from the liquid surface.

4. In spite of efforts to minimize effects of the liquid phase, by using a small measuring volume and phase discrimination, and the fact that the multiphase mixing layer appears to be instantaneously dilute, only the outer half of the multiphase mixing layer was accessible to measurements of gas velocities using laser velocimetry. In contrast, double-pulse holography provided access to the flow up to the liquid surface, although improvements of this technique are needed so that drops having diameters smaller than 5 μm (which would provide better response to gas motion) can be observed with more efficient methods of data reduction.

Residence-time considerations discussed in this paper are only provisional pending additional experimental evaluation. Nevertheless, these considerations show that dense-spray properties and the relative importance of particular phenomena vary widely with experimental conditions. Thus, flow properties should be considered on a case-by-case basis and generalizations obtained from particular data sets should be accepted with caution. Clearly, additional data are needed in order to gain a better understanding of the dense spray region of pressure-atomized sprays.

Acknowledgements

This research was sponsored by the Air Force Office of Scientific Research Grant Nos. AFOSR 85-0244 and 89-0516; and by the Office of Naval Research, Grant No. N00014-89-J-1199. The U.S. Government is authorized to reproduce and distribute copies for Governmental purposes notwithstanding any copyright notation thereon.

References

[1]Ruff, G. A., Bernal, L. P. and Faeth, G. M., "Structure of the Near-Injector Region of Non-Evaporating Pressure-Atomized Sprays," AIAA Paper No. 89-0050, 1989; also, J. Propulsion and Power, submitted.

[2]Ruff, G. A., Sagar, A. D. and Faeth, G. M., "Structure and Mixing Properties of Pressure-Atomized Sprays," *AIAA Journal*, Vol. 27, July 1989, pp. 901-908.

[3]Ranz, W. E., "Some Experiments on Orifice Sprays," *Can J. Chem. Engr.*, Vol. 36, August 1958, pp. 175-181.

[4]Miesse, C. C., "Correlation of Experimental Data on Disintegration of Liquid Jets," *Ind. Engr. Chem.*, Vol. 47, September 1955, pp. 1690-1697.

[5]Faeth, G. M., "Mixing, Transport and Combustion in Sprays," *Prog. Energy Combust. Sci.*, Vol. 13, 1987, pp. 293-345.

[6]Phinney, R. E., "The Breakup of a Turbulent Liquid Jet in a Gaseous Atmosphere," *J. Fluid Mech.*, Vol. 60, October 1973, pp. 689-701.

[7]Hiroyasu, H., Shimizu, M. and Arai, M., "The Breakup of a High Speed Jet in a High Pressure Gaseous Environment," ICLASS-82, University of Wisconsin, Madison, Wisconsin, 1982.

[8]Chehroudi, B., Onuma, Y., Chen, S.-H. and Bracco, F. V., "On the Intact Core of Full-Cone Sprays," SAE Paper No. 850126, 1985.

[9]Wu, K.-J., Su, C.-C., Steinberger, R. L., Santavicca, D. A. and Bracco, F. V., "Measurements of the Spray Angle of Atomizing Jets," *J. Fluids Engr.*, Vol. 105, December 1983, pp. 406-415.

[10]Wu, K.-J., Coghe, A., Santavicca, D. A. and Bracco, F. V., "LDV Measurements of Drop Velocity in Diesel-Type Sprays," *AIAA Journal*, Vol. 22, September 1984, pp. 1263-1270.

[11]Mao, C.-P., Wakamatsu, Y. and Faeth, G. M., "A Simplified Model of High Pressure Spray Combustion," *Eighteenth Symposium (International) on Combustion*, The Combustion Institute, Pittsburgh, 1980, pp. 337-347.

[12]Bracco, F. V., "Structure of High-Speed Full-Cone Sprays," *Recent Advances in Gas Dynamics* (C. Casci, ed.), Plenum Publishing Corp., New York, 1983.

[13]Ruff, G. A., "Structure and Mixing Properties of the Near-Injector Region of Nonevaporating Pressure-Atomized Sprays," Ph.D. Thesis, University of Michigan, Ann Arbor, Michigan, 1990.

[14]Hinze, J. O., *Turbulence*, 2nd ed., McGraw-Hill, New York, 1975, p. 427 and pp. 724-734.

[15]Schlichting, H., *Boundary Layer Theory*, 7th ed., McGraw-Hill, New York, 1979, p. 599.

[16]Modarress, D., Tan, H. and Elgobashi, S., "Two-Component LDA Measurements in a Two-Phase Turbulent Jet," *AIAA Journal*, Vol. 22, May 1984, pp. 624-630.

[17]Trolinger, J. O., "Laser Instrumentation for Flow Field Diagnostics," AGARD-AG-186, NATO, Paris, 1977, pp. 59-89.

[18]Lockwood, F. C. and Naguib, A. S., "The Prediction of Fluctuations in the Properties of Free, Round-Jet Turbulent Diffusion Flames," *Combust. Flame*, Vol. 24, February 1975, pp. 109-124.

[19]Bilger, R. W., "Turbulent Jet Diffusion Flames," *Prog. Energy Combust. Sci.*, Vol. 1, 1976, pp. 87-109.

[20]Jeng, S.-M. and Faeth, G. M., "Species Concentrations and Turbulence Properties in Buoyant Methane Diffusion Flames," *J. Heat Trans.*, Vol. 106, August 1985, pp. 721-727.

[21]Loth, E. and Faeth, G. M., "Structure of Underexpanded Round Air Jets Submerged in Water," *Int. J. Multiphase Flow*, Vol. 15, 1989, pp. 589-603.

[22]Solomon, A.S.P., Shuen, J.-S., Zhang, Q.-F. and Faeth, G. M., "Structure of Nonevaporating Sprays: I. Near-Injector Conditions and Mean Properties," *AIAA Journal*, Vol. 23, October 1985, pp. 1548-1555.

[23]Solomon, A.S.P., Shuen, J.-S., Zhang, Q.-F. and Faeth, G. M., "Structure of Nonevaporating Sprays: II. Drop and Turbulence Properties," *AIAA Journal*, Vol. 23, November 1985, pp. 1724-1730.

[24]Reitz, R. D., "Atomization and Other Breakup Regimes of a Liquid Jet," Ph.D. Dissertation No. 1375-T, Princeton University, Princeton, New Jersey, 1978.

[25]Reitz, R. D. and Bracco, F. V., "Mechanism of Atomization of Liquid Jets," *Phys. Fluids*, Vol. 25, October 1982, pp. 1730-1742.

[26]Taylor, G. C., "Generation of Ripples by Wind Blowing Over a Viscous Liquid," *Collected Works of G. I. Taylor 3*, 1940, pp. 244-254.

[27]Clift, R., Grace, J. R. and Weber, M. E., *Bubbles, Drops and Particles*, Academic Press, New York, 1978, p. 346.

[28]Pruppacker, H. R. and Klett, J. D., *Microphysics of Clouds and Precipitation*, D. Reidel Publishing Co., Boston, 1978, pp. 123-456.

[29]Ranger, A. A. and Nicholls, J. A., "Aerodynamic Shattering of Liquid Drops," *AIAA Journal*, Vol. 7, February 1969, pp. 285-290.

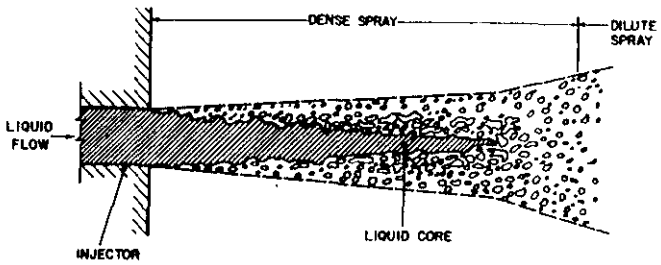

Fig. 1 Sketch of the near-injector region for pressure-atomized injection and atomization breakup.

Table 1 Drop sizes near the liquid surface

x/d	Slug Flow			Fully-Developed Flow		
	u_{gs}(m/s)[a]	SMD(μm)[b]	$d_{p_{av}}$(m/s)[c]	u_{gs}(m/s)[a]	SMD(μm)[b]	$d_{p_{av}}$(m/s)[c]
12.5	3	170	210	10	1020	270
25	3	140	200	8	940	250
50	9	480	260	15	1400	340
100	6	220	240	9	1690	260

[a]Gas velocity estimated from 5 μm diameter drops near surface.

[b]Measured SMD from Ruff et al.[1]

[c]Average drop diameter near liquid surface from aerodynamic breakup theory for a liquid velocity, u_o = 56.3 m/s, and C_B = 0.5.

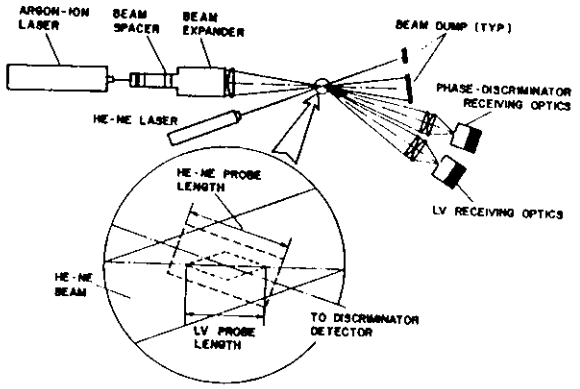

Fig. 2 Sketch of the phase discriminating laser-velocimetry system.

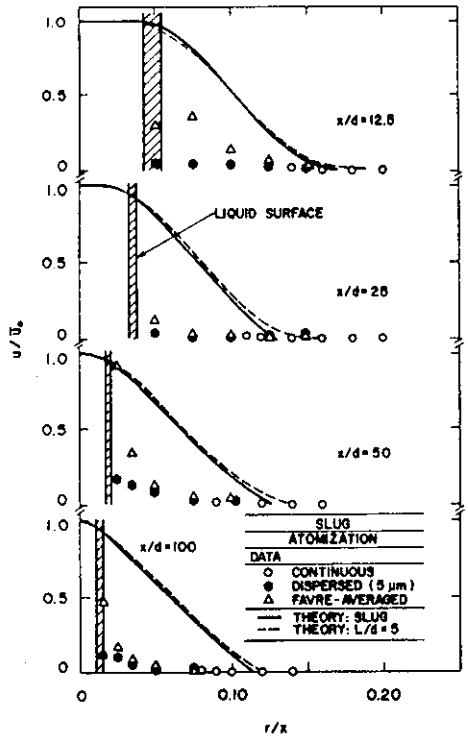

Fig. 3 Mean phase velocities for slug flow and atomization breakup.

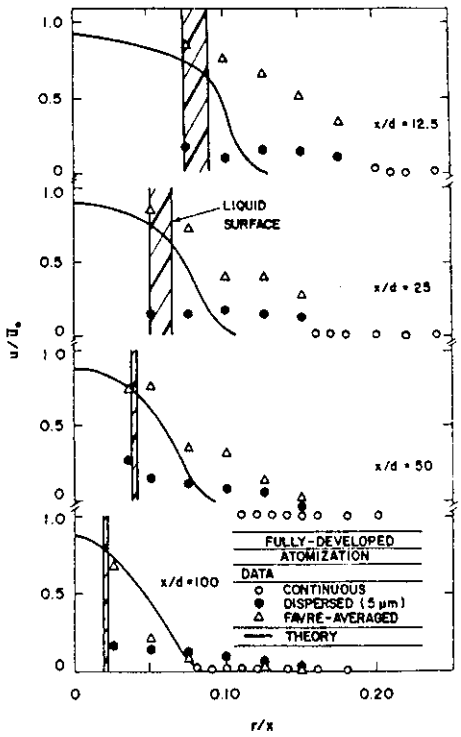

Fig. 4 Mean phase velocities for fully-developed flow and atomization breakup.

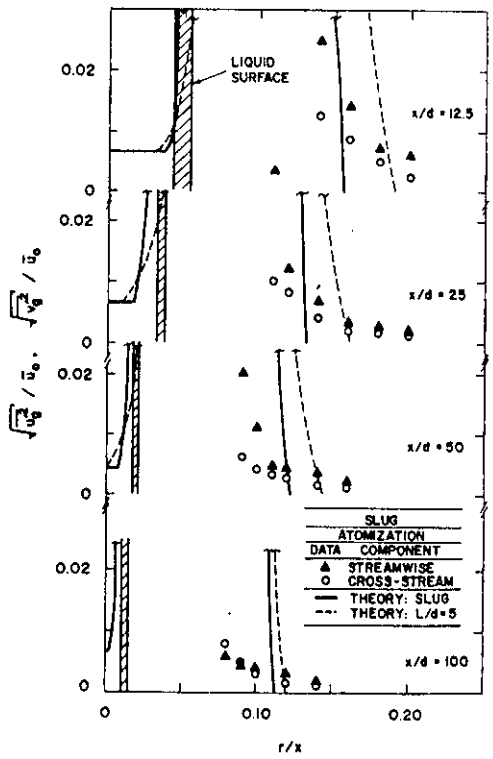

Fig. 5 Gas-phase velocity fluctuations for slug flow and atomization breakup.

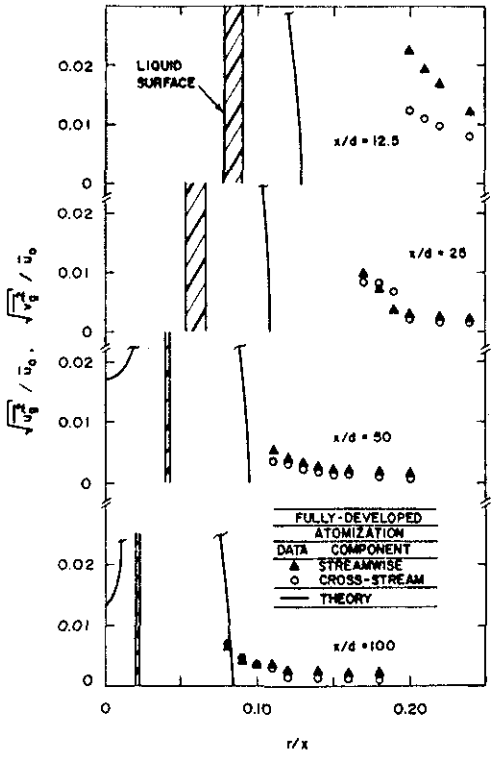

Fig. 6 Gas-phase velocity fluctuations for fully-developed flow and atomization breakup.

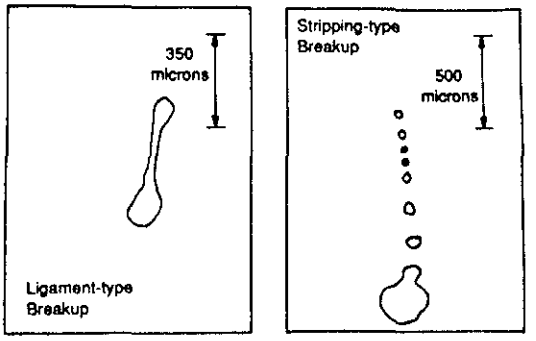

Fig. 8 Sketches of stripping and ligament secondary drop breakup in the mixing layer.

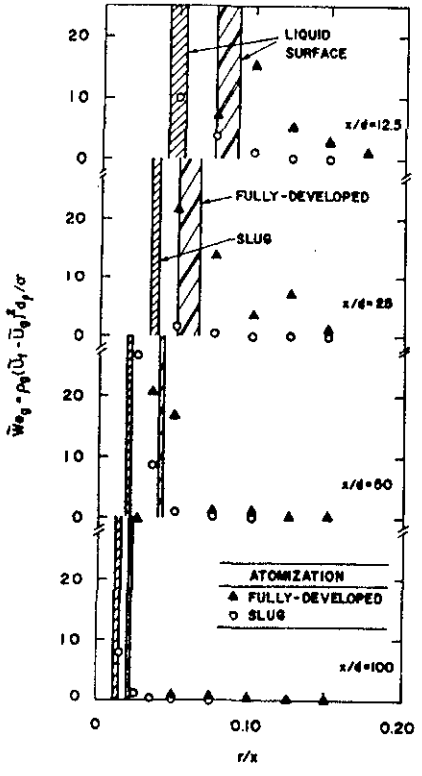

Fig. 7 Favre-averaged Weber numbers for slug and fully-developed flow and atomization breakup.

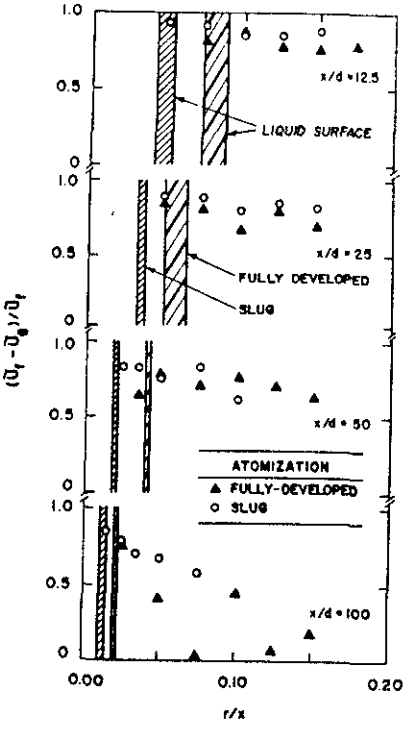

Fig. 9 Favre-averaged separated-flow factor for slug and fully-developed flow and atomization breakup.